Dimensionality reduction and density-based clustering for transfer function design in Direct Volume Rendering

SIBGRAPI Paper ID: 99999

***Abstract*—Transfer functions (TFs) are a fundamental component of volume visualization and have been extensively studied in the context of Direct Volume Rendering (DVR). In the traditional DVR pipeline, TFs serve multiple roles, primarily material classification and mapping data values to optical properties. The effectiveness of a TF is closely tied to the characteristics of the underlying data. While multidimensional TFs offer increased classification capabilities, their design remains a complex task, especially when aiming to emphasize specific volume features. This paper presents an unsupervised volume classification method that facilitates both the definition and design of TFs. The proposed approach combines dimensionality reduction, clustering and pivot-based indexing to support the specification of meaningfulTFs. The results include a user-friendly volume exploration workflow based on initial TF parameters, a semi-automated classification mechanism, and an enhanced 2D scatterplot interface for interactive data analysis.**

I. Introduction

Direct Volume Rendering (DVR) is widely used in scientific and medical applications to visualize three-dimensional scalar data. A key element in DVR is the transfer function (TF), which maps volume data attributes (e.g., density) to visual properties such as color and opacity [1].

Multidimensional TFs can enhance data classification, but their design becomes increasingly complex with more input attributes [1], [2]. Since no universal TF fits all datasets, design is often manual and highly dependent on user expertise [3]. Dimensionality and non-intuitive parameter spaces further complicate the process.

We propose a low-cost, unsupervised approach to simplify TF design. Our method combines clustering, dimensionality reduction, and pivot-based indexing to support semi-automated classification. A modified 2D scatter plot interface facilitates intuitive exploration of volume features.

Our main contributions are:

- A computationally efficient method for generating TFs with minimal manual adjustment.
- A user-friendly exploration interface for interacting with classified volume data.

The remainder of this paper is organized as follows: Section II reviews related work; Section III presents our method; Section IV describes the exploration interface; results and discussion are given in Sections V and VI; and Section VII concludes the paper.

II. Related Works

Various aspects of transfer functions (TFs) have been extensively discussed in the literature [1]. Our review focuses on methods that support user interaction in multidimensional TF design, particularly those employing machine learning, dimensionality reduction, and information visualization techniques.

A typical multidimensional TF incorporates either multivariate or derived input data. Multivariate attributes originate from the volume acquisition process, while derived attributes are computed from primary data, such as density. The gradient is the most commonly used derived attribute, but others include curvature, size, distance, texture and statistical measures.

Selecting an optimal subset of attributes to maximize material classification accuracy is a complex task. [3] argue that no single TF design is universally effective. Considering all available attributes is impractical, as it may increase computational costs and introduce noise, degrading classification performance. This classical challenge is known as the "curse of dimensionality." Dimensionality reduction is the most common approach to address this issue and several studies have applied such techniques to multidimensional TF design [4]–[8].

Histograms are commonly used as componente for 2D TFs design [9], typically representing intensity–gradient magnitude or low–high histograms. Several approaches have been proposed to automate histogram-based TF design. Röttger et al. [10] group spatially connected regions and associate gradient values with spatial coordinates to classify datasets. Many methods combine histograms with clustering algorithms, including affinity propagation [11], hierarchical clustering [12], and iterative self-organizing data analysis [13].

Approaches to multidimensional TF design generally follow two main strategies. The first provides an interface that allows users to manipulate all data attributes—such as the parallel coordinate plot (PCP). The second applies dimensionality reduction techniques, such as Multidimensional Scaling (MDS) or Principal Component Analysis (PCA), to create simplified visual representations.

[14] employed PCP in their exploration scheme, integrating viewer parameters and TF specification into the interface. [8] followed a similar approach, applying a local linear embedding technique for dimensionality reduction. Likewise, [15] proposed a hybrid interface that combines PCP with a scatter plot generated using MDS.

[7] applied a Self-Organizing Map (SOM) and a radial basis function for TF design. SOM performs unsupervised

learning to reduce dimensionality, producing a map in which neighboring regions represent similar voxels. Users interact with the map by drawing widgets in specific regions. [16] extended this idea using a spherical SOM, enabling interaction on a spherical lattice. [17] proposed a volume exploration space based on subtree structures derived from hierarchical clustering and modified dendrograms. Later, [4] revisited these ideas, augmenting SOM with a normalized cut step to create a "cell map," in which each region encodes volume information tied to meaningful structures. Our method shares similarities with the work of [4], but employs an MDS-based technique and a density-based clustering algorithm to automate material classification, resulting in a modified scatter plot view.

[18] proposed one of the earliest TF design strategies using supervised learning, implementing neural networks and support vector machines. [19] combined SOM with back-propagation neural networks for material classification. [20] used a Generative Adversarial Network (GAN) framework to compute models for TF specification and view selection. More recently, [21] combined GANs with Convolutional Neural Networks (CNNs) to synthesize the exploration process. [22] developed a method using CNNs to generate visualizations from TF colorizations. [2] introduced a deep learning-based gallery approach with differentiable rendering to support user exploration of the design space.

[23] proposed a graph-based method for identifying significant volume structures, which involves clustering features, building a material graph topology, and enhancing the rendering of important structures.

III. Method

This section presents our unsupervised method for TF design, enabling semi-automated material classification and initial TF specification for intuitive volume exploration.

Fig. 1 shows an overview. After organizing the dataset into a volume grid, we apply three steps: dimensionality reduction, clustering, and pivot-based indexing.

A. Dimensionality Reduction

We use FastMap [24] to project high-dimensional data into 2D while preserving clustering structure. The algorithm finds two distant pivots and projects points onto the line between them.

Let d be the number of attributes and n the number of voxels. The steps are:

1) Find two points (pivots) furthest apart.
2) Project points onto a hyperplane orthogonal to the pivots' line.

To avoid quadratic complexity, we use the heuristic from [24] (Algorithm 1) which approximates distant pivots.

Time complexity is $\mathcal{O}(nk)$ with $k = 2$.

Algorithm 1: Pivot searching of FastMap.

Input: $\mathbb{O}$
Output: Pivots O_a, O_b
$O_a \leftarrow$ random point $o \in \mathbb{O}$
$O_b \leftarrow$ point $o \in \mathbb{O}$ farthest from O_a
$O_a \leftarrow$ point $o \in \mathbb{O}$ farthest from O_b

B. Clustering

A major goal of our method is to simplify material classification and facilitate the highlighting of volume details. We address this objective by employing a classical density-based clustering algorithm, the DBSCAN [25].

DBSCAN is a widely utilized algorithm known for its success across various applications [26]. Nevertheless, its adoption in DVR comes with some caveats. The original version [25] exhibits a time complexity of $\mathcal{O}(n^2)$ in the worst case [26]. With practical usability in mind, we implemented a grid-based DBSCAN proposed by [27]. This version claims a time complexity of $\mathcal{O}(n \log(n))$.

Like the original algorithm [25], the 2D grid version also has $minPts$ and ε as input parameters. In this way, the user must fine-tune such parameters to best classify the volume data.

When this method step ends, each cluster comprises a subset of voxels that potentially represent a region of interest.

[27] introduces the concept of a grid to improve the efficiency of the clustering process, especially for high-dimensional datasets. The authors improve the scalability and efficiency of traditional DBSCAN by leveraging grid-based partitioning and density estimation techniques. Detailed explanations are provided in the works of [27] and [28]. The algorithm operates on a cell grid and comprises the tasks summarized next.

1) Grid partitioning. The first step involves partitioning the space into a grid of cells. Each cell represents a small portion of the entire space.
2) Density estimation. Within each cell, the algorithm calculates the density of points. The density is usually estimated using a distance threshold (ε) to determine the neighborhood of each point.
3) Identifying core points. Points with a density above a certain threshold ($minPts$) are considered core points. These core points are potential seeds for clusters.
4) Expanding clusters. Starting from a core point, the algorithm expands the cluster by iteratively adding neighboring points that also qualify as core points. The expansion continues until there are no more core points to be added.
5) Handling border points. Points that are within the ε neighborhood of a core point but do not meet the density requirement to be considered core themselves are classified as border points. Border points are assigned to the cluster of their nearest core point.
6) Handling noise. The points that are not core and do not belong to any cluster are considered noise points.

Fig. 1. Overview of the proposed unsupervised method for transfer function definition and design.

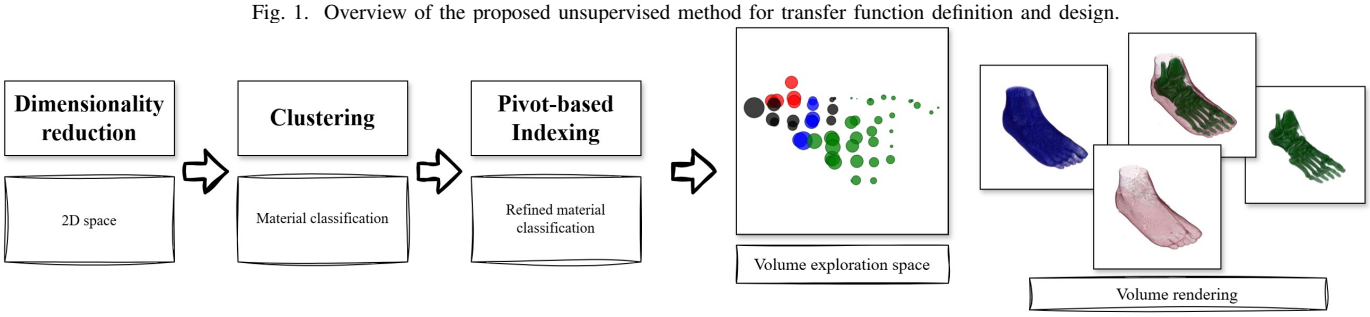

C. Pivot-based indexing

To reduce scatter plot clutter, we plot only selected pivots within each cluster. Each cluster is subdivided into sub-clusters by assigning points to their nearest pivot (Algorithm 2).

Algorithm 2: Finding sub-clusters within a cluster.

Input: Points $\mathbb{P}$ of cluster c
Input: Pivots $\mathbb{P}_s$ of cluster c
Output: Points with sub-cluster assignment
foreach $p \in \mathbb{P}$ **do**
  $p_s \leftarrow$ nearest pivot in $\mathbb{P}_s$
  Assign p to p_s's sub-cluster
end

We select pivots using Sparse Spatial Selection (SSS) [29], which adds points as pivots if they are sufficiently distant from existing ones, controlled by a distance factor α.

Algorithm 3: Sparse Spatial Selection.

Input: Points $\mathbb{P}$
Output: Selected pivots $\mathbb{P}_s$
$\mathbb{P}_s \leftarrow \{p_1\}$
foreach $p \in \mathbb{P}$ **do**
  if $\forall p_s \in \mathbb{P}_s, dist(p, p_s) \geq M\alpha$ **then**
    $\mathbb{P}_s \leftarrow \mathbb{P}_s \cup \{p\}$
  end
end

Adjusting α controls the number of pivots: smaller α selects more pivots; values near 1 select fewer.

IV. Volume Exploration Space

Figure 2 illustrates the TF design interface, a 2D scatter plot where each circle represents a pivot selected by SSS. The positions from FastMap determine the points' coordinates. Each pivot is a central point of a cluster, with its circle radius proportional to the number of voxels it represents, normalized logarithmically.

Our method generates an initial TF specification using a predefined opacity and a rainbow color scale, assigning a unique color per cluster.

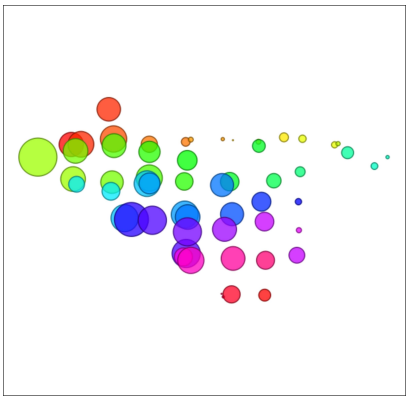

(a) Initial transfer function specification (semi-automatic generated).

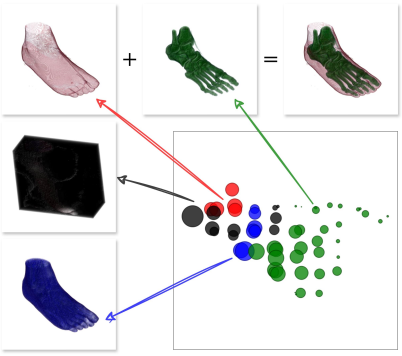

(b) Fine-tune material classification after user adjustment.

Fig. 2. Transfer function design interface and volume exploration space of a right male foot dataset.

Users adjust the TF following the WYSIWYG principle: pivot color and opacity map directly to their associated voxels according to clustering. Both selected and unselected elements can be customized.

Volume exploration occurs through pivot selection. The system dynamically increases the opacity of selected pivots and decreases that of others. Users can make arbitrary selections, save them as groups, and interact with pivots, clusters, or groups as selectable entities.

Iterative selection of nearby elements aids identifying volume details. FastMap and DBSCAN naturally cluster similar

instances spatially, simplifying this process.

Our approach automates material classification by assuming each cluster or pivot represents a relevant item. If unsatisfied, users may select/deselect elements or adjust parameters:

- input volume data,
- DBSCAN parameters ε and $minPts$,
- SSS distance factor α.

V. Results

A. Experimental Design

Experiments ran on an Intel Core i5-7200U, 8 GB RAM, Ubuntu 22.04 64-bit, with an NVIDIA GeForce GT 940MX GPU.

We used classical volume ray-casting with Blinn-Phong illumination and trilinear interpolation. Ray step adjusted per voxel spacing. Runtimes are averages of five trials.

The system was implemented in C++ using Qt and CUDA C/C++. The implementation is publicly available.

Table I lists the volume datasets used in experiments.

All volumes contain scalar density values. Multidimensional attributes were derived—13 in total—including intensity, gradient magnitude, Laplacian magnitude, and 10 local histogram statistics (absolute deviation, contrast, energy, entropy, inertia, kurtosis, mean, skewness, standard deviation, variance).

Attribute selection was empirical, tailored per dataset to balance discrimination and computational cost.

TABLE I
VOLUME DATASETS.

Dataset	Grid size	Total voxels
Engine block	$256 \times 256 \times 256$	16,777,216
Knees	$379 \times 229 \times 305$	26,471,255
Tooth	$256 \times 256 \times 161$	10,551,296

B. Runtime

Table II presents runtimes (seconds) for each dataset.

TABLE II
RUNTIME (SECONDS) OF THE PROPOSED METHOD PER DATASET.

	Engine block	Knees	Tooth
Dimensionality reduction	7.50	7.98	36.05
Clustering	51.52	102.77	19.42
Pivot-based indexing	2.23	3.15	1.33
Volume exploration space	1.48	1.86	0.79

C. Data classification

Attribute selection was done empirically by iterative testing and visual assessment, ensuring effective separation of volumetric structures while maintaining computational feasibility.

DBSCAN's $minPts$ was fixed at 4 [25]. Parameter ε varied within $[0.2, 0.35]$, and SSS parameter α within $[0.8, 0.95]$ for volume exploration.

1) Engine block dataset: Figure 3 shows the volume exploration space for the engine block. Each numbered group corresponds to classified volume details in Fig. 4. Parameters: $k = 4$, TF = {intensity, skewness, gradient magnitude, variance}; $minPts = 4$; $\varepsilon = 0.35$; $\alpha = 0.85$.

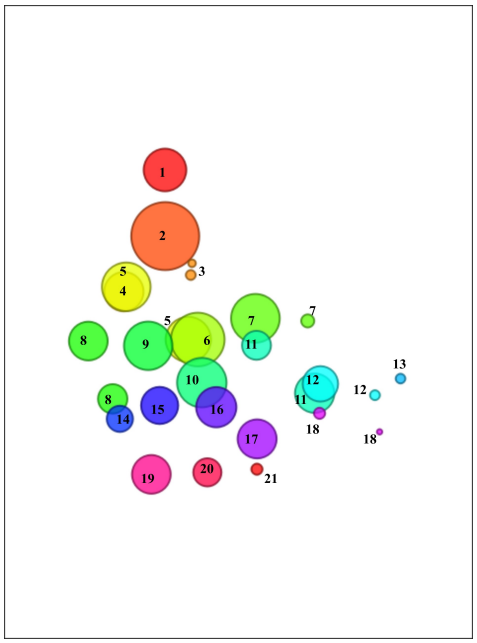

Fig. 3. Volume exploration space for engine block dataset. Parameters: TF = {intensity, skewness, gradient magnitude, variance}; $minPts = 4$; $\varepsilon = 0.35$; $\alpha = 0.85$.

Figure 5 shows a volume exploration simulation revealing engine components, starting from Fig. 3.

2) Knees dataset: Preliminary classification is shown in Fig. 6 with rendered details in Fig. 7. Parameters: TF = {intensity, variance, absolute deviation, energy, contrast}; $minPts = 4$; $\varepsilon = 0.35$; $\alpha = 0.9$.

Figure 8 illustrates grouped bones and muscles: femur, tibia, patella, fibula, thigh and knee muscles.

3) Tooth dataset: Figure 10 shows the volume exploration space, with rendered details in Fig. 10. Parameters: TF = {intensity, variance, absolute deviation, energy, contrast, entropy}; $minPts = 4$; $\varepsilon = 0.23$; $\alpha = 0.9$.

Figure 11 shows empirically grouped tooth structures: enamel, pulp, dentin, crown, entire tooth, and immersion fluid.

VI. Discussion

The dimensionality reduction approach effectively addresses common challenges in transfer function design by simplifying the data representation. The choice of DBSCAN parameters strongly affects classification outcomes. The $minPts$ parameter can reliably use a default value of 4 [25], given that FastMap reduces the data to a 2D space. However, the ε parameter requires careful tuning: larger values produce fewer but larger clusters, while smaller values result in more numerous, smaller clusters.

Fig. 4. Rendered classified volume details for engine block. Parameters as in Fig. 3.

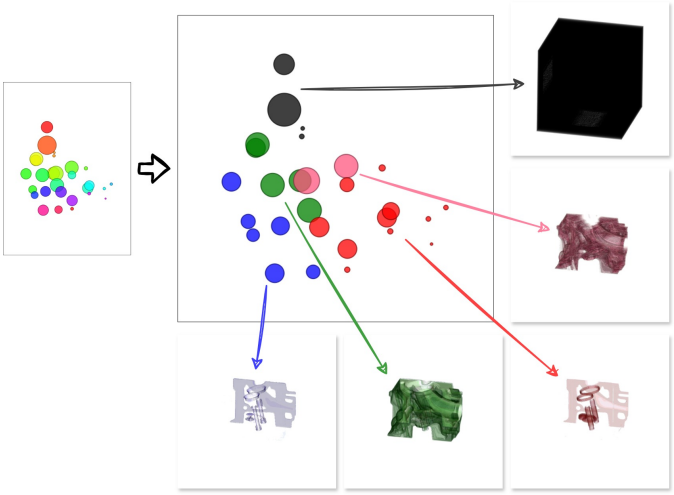

Fig. 5. User-refined transfer function and volume classification for engine block. Groups formed empirically. Parameters as in Fig. 3.

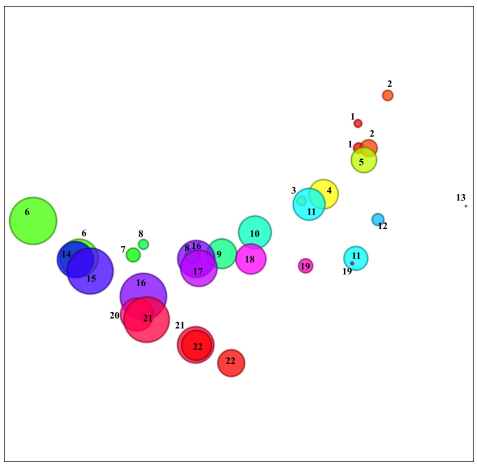

Fig. 6. Volume exploration space for knees dataset. Parameters as above.

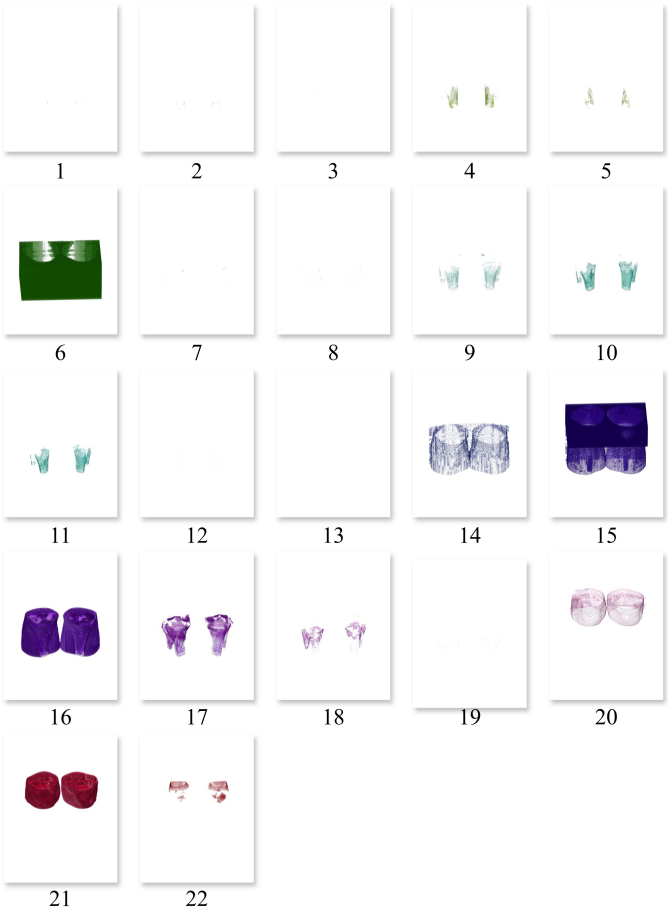

Fig. 7. Rendered classified volume details for knees dataset. Parameters as above.

The SSS distance factor (α) similarly influences clustering granularity, varying inversely with the number of pivots per cluster.

Overall, the method incurs minimal computational overhead, demonstrating efficient performance and promising scalability for large volumetric datasets.

VII. Conclusions

We presented a robust method for transfer function (TF) design that integrates feature classification with a simplified volume exploration space. Our approach combines FastMap for efficient feature extraction, DBSCAN for effective clus-

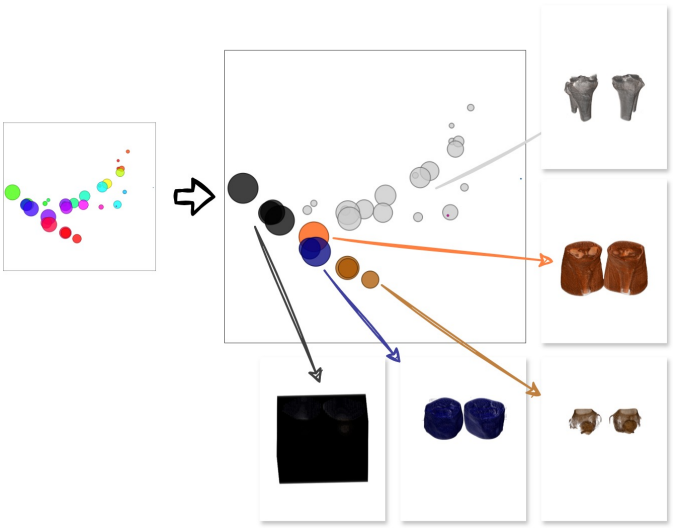

Fig. 8. User-refined TF and classification for knees dataset. Groups formed empirically. Parameters as above.

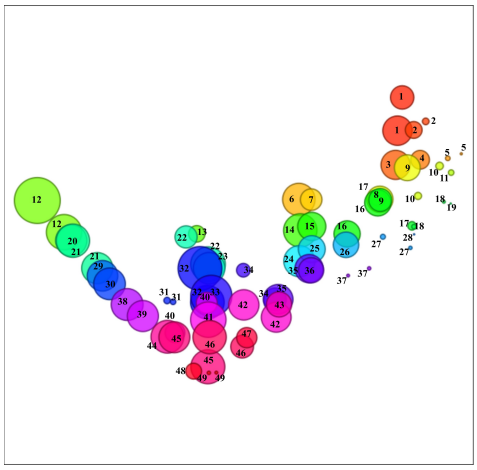

Fig. 9. Volume exploration space for tooth dataset. Parameters as above.

tering, and SSS for pivot-based indexing. These techniques enable semi-automatic classification and initial TF specification, visualized through an intuitive scatter plot interface for volume exploration.

The method exhibits low computational overhead, short runtimes, and minimal storage requirements, highlighting its practicality and scalability for real-world applications. Future work will focus on assessing the method's performance with large, high-dimensional datasets to validate its scalability and effectiveness.

Moreover, we aim to extend our evaluation to multivariate data, enhancing the method's applicability and robustness across a wider range of volume datasets.

Acknowledgements

This work was partially supported by the Brazilian Coordenação de Aperfeiçoamento de Pessoal de Nível Superior (CAPES).

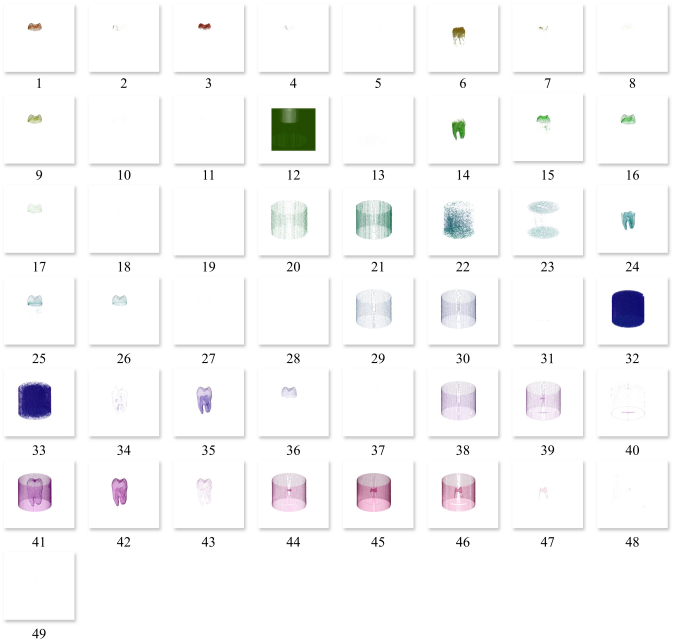

Fig. 10. Rendered classified volume details for tooth dataset. Parameters as above.

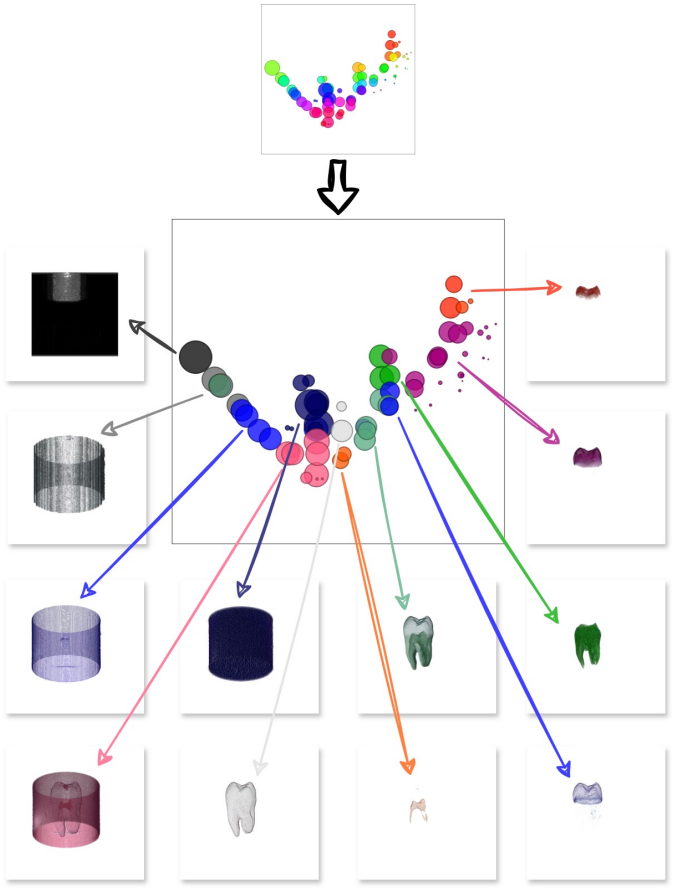

Fig. 11. User-refined TF and classification for tooth dataset. Groups formed empirically. Parameters as above.

REFERENCES

[1] P. Ljung, J. Krüger, E. Groller, M. Hadwiger, C. D. Hansen, and A. Ynnerman, "State of the art in transfer functions for direct volume rendering," in *Computer graphics forum*, vol. 35, no. 3. Wiley Online Library, 2016, pp. 669–691.

[2] B. Pan, J. Lu, H. Li, W. Chen, Y. Wang, M. Zhu, C. Yu, and W. Chen, "Differentiable design galleries: A differentiable approach to explore the design space of transfer functions," *IEEE Transactions on Visualization and Computer Graphics*, vol. 30, no. 1, pp. 1369–1379, 2024.

[3] S. Arens and G. Domik, "A survey of transfer functions suitable for volume rendering." in *VG@ Eurographics*, 2010, pp. 77–83.

[4] L. Cai, B. P. Nguyen, C.-K. Chui, and S.-H. Ong, "A two-level clustering approach for multidimensional transfer function specification in volume visualization," *Vis. Comput.*, vol. 33, no. 2, p. 163–177, feb 2017. [Online]. Available: https://doi.org/10.1007/s00371-015-1167-y

[5] A. Abbasloo, V. Wiens, M. Hermann, and T. Schultz, "Visualizing tensor normal distributions at multiple levels of detail," *IEEE Transactions on Visualization and Computer Graphics*, vol. 22, no. 1, pp. 975–984, 2016.

[6] Y. Gao, C. Chang, X. Yu, P. Pang, N. Xiong, and C. Huang, "A vr-based volumetric medical image segmentation and visualization system with natural human interaction," *Virtual Real.*, vol. 26, no. 2, p. 415–424, jun 2022. [Online]. Available: https://doi.org/10.1007/s10055-021-00577-4

[7] F. D. M. Pinto and C. M. D. S. Freitas, "Design of multi-dimensional transfer functions using dimensional reduction," in *Proceedings of the 9th Joint Eurographics/IEEE VGTC conference on Visualization*, 2007, pp. 131–138.

[8] X. Zhao and A. Kaufman, "Multi-dimensional reduction and transfer function design using parallel coordinates," in *Volume graphics. International Symposium on Volume Graphics*. NIH Public Access, 2010, p. 69.

[9] J. Kniss, G. Kindlmann, and C. Hansen, "Multidimensional transfer functions for interactive volume rendering," *IEEE Transactions on visualization and computer graphics*, vol. 8, no. 3, pp. 270–285, 2002.

[10] S. Roettger, M. Bauer, and M. Stamminger, "Spatialized transfer functions," in *Proceedings of the Seventh Joint Eurographics / IEEE VGTC Conference on Visualization*, ser. EUROVIS'05. Goslar, DEU: Eurographics Association, 2005, p. 271–278.

[11] T. Zhang, Z. Yi, J. Zheng, D. C. Liu, W.-M. Pang, Q. Wang, J. Qin *et al.*, "A clustering-based automatic transfer function design for volume visualization," *Mathematical Problems in Engineering*, vol. 2016, 2016.

[12] P. Sereda, A. Vilanova, and F. A. Gerritsen, "Automating transfer function design for volume rendering using hierarchical clustering of material boundaries." in *EuroVis*, 2006, pp. 243–250.

[13] F.-Y. Tzeng and K.-L. Ma, "A cluster-space visual interface for arbitrary dimensional classification of volume data," in *Proceedings of the Sixth Joint Eurographics - IEEE TCVG Conference on Visualization*, ser. VISSYM'04. Goslar, DEU: Eurographics Association, 2004, p. 17–24.

[14] M. Tory, S. Potts, and T. Moller, "A parallel coordinates style interface for exploratory volume visualization," *IEEE Transactions on Visualization and Computer Graphics*, vol. 11, no. 1, pp. 71–80, 2005.

[15] H. Guo, H. Xiao, and X. Yuan, "Multi-dimensional transfer function design based on flexible dimension projection embedded in parallel coordinates," in *2011 IEEE Pacific Visualization Symposium*. IEEE, 2011, pp. 19–26.

[16] N. M. Khan, M. Kyan, and L. Guan, "Intuitive volume exploration through spherical self-organizing map and color harmonization," *Neurocomputing*, vol. 147, pp. 160–173, 2015.

[17] L. Wang, X. Zhao, and A. E. Kaufman, "Modified dendrogram of attribute space for multidimensional transfer function design," *IEEE transactions on visualization and computer graphics*, vol. 18, no. 1, pp. 121–131, 2011.

[18] F.-Y. Tzeng, E. B. Lum, and K.-L. Ma, "An intelligent system approach to higher-dimensional classification of volume data," *IEEE Transactions on visualization and computer graphics*, vol. 11, no. 3, pp. 273–284, 2005.

[19] L. Wang, X. Chen, S. Li, and X. Cai, "General adaptive transfer functions design for volume rendering by using neural networks," in *International Conference on Neural Information Processing*. Springer, 2006, pp. 661–670.

[20] M. Berger, J. Li, and J. A. Levine, "A generative model for volume rendering," *IEEE transactions on visualization and computer graphics*, vol. 25, no. 4, pp. 1636–1650, 2018.

[21] F. Hong, C. Liu, and X. Yuan, "Dnn-volvis: Interactive volume visualization supported by deep neural network," in *2019 IEEE Pacific Visualization Symposium (PacificVis)*. IEEE, 2019, pp. 282–291.

[22] S. Kim, Y. Jang, and S.-E. Kim, "Image-based tf colorization with cnn for direct volume rendering," *IEEE Access*, vol. 9, pp. 124 281–124 294, 2021.

[23] O. Sharma, T. Arora, and A. Khattar, "Graph-based transfer function for volume rendering," in *Computer Graphics Forum*, vol. 39, no. 1. Wiley Online Library, 2020, pp. 76–88.

[24] C. Faloutsos and K.-I. Lin, "Fastmap: A fast algorithm for indexing, data-mining and visualization of traditional and multimedia datasets," in *Proceedings of the 1995 ACM SIGMOD international conference on Management of data*, 1995, pp. 163–174.

[25] M. Ester, H.-P. Kriegel, J. Sander, X. Xu *et al.*, "A density-based algorithm for discovering clusters in large spatial databases with noise," in *kdd*, vol. 96, no. 34, 1996, pp. 226–231.

[26] E. Schubert, J. Sander, M. Ester, H. P. Kriegel, and X. Xu, "Dbscan revisited, revisited: why and how you should (still) use dbscan," *ACM Transactions on Database Systems (TODS)*, vol. 42, no. 3, pp. 1–21, 2017.

[27] A. Gunawan and M. de Berg, "A faster algorithm for dbscan," *Master's thesis*, 2013.

[28] J. Gan and Y. Tao, "Dbscan revisited: Mis-claim, un-fixability, and approximation," in *Proceedings of the 2015 ACM SIGMOD international conference on management of data*, 2015, pp. 519–530.

[29] O. Pedreira and N. R. Brisaboa, "Spatial selection of sparse pivots for similarity search in metric spaces," in *International Conference on Current Trends in Theory and Practice of Computer Science*. Springer, 2007, pp. 434–445.